Journal of Oceanology and Limnology
Vol. 42, No. 4, pp. 1019-1036, 2024
https://doi.org/10.1007/s00343-023-3129-y

Research Paper

Salinity effect-induced ENSO amplitude modulation in association with the interdecadal Pacific Oscillation*

Hai ZHI[1], Xiaokun WANG[1], Rong-Hua ZHANG[2, 3, **], Pengfei LIN[4], Jifeng QI[3, 5]

[1] *College of Atmospheric Sciences, Nanjing University of Information Science and Technology, Nanjing 210044, China*
[2] *School of Marine Sciences, Nanjing University of Information Science and Technology, Nanjing 210044, China*
[3] *Laoshan Laboratory, Qingdao 266237, China*
[4] *State Key Laboratory of Numerical Modeling for Atmospheric Sciences and Geophysical Fluid Dynamics (LASG), Institute of Atmospheric Physics (IAP), Chinese Academy of Sciences, Beijing 100029, China*
[5] *Key Laboratory of Ocean Circulation and Waves, Institute of Oceanology, and Center for Ocean Mega-Science, Chinese Academy of Sciences, Qingdao 266071, China*

Received Jul. 3, 2023; accepted in principle Sep. 12, 2023; accepted for publication Nov. 3, 2023

Abstract A 110-year ensemble simulation of an ocean general circulation model (OGCM) was analyzed to identify the modulation of salinity interdecadal variability on El Niño-Southern Oscillation (ENSO) amplitude in the tropical Pacific during 1901–2010. The simulating results show that sea surface salinity (SSS) variation in the region exhibits notable and coherent interdecadal variability signal, which is closely associated with the Interdecadal Pacific Oscillation (IPO). As salinity increases or reduces, the SSS modulations on ENSO amplitude during its warm/cold events vary asymmetrically with positive/negative IPO phases. Physically, salinity interdecadal variability can enhance or reduce ENSO-related conditions in upper-ocean stratification, contributing noticeably to ENSO variability. Salinity anomalies associated with the mixed layer depth and barrier layer thickness can modulate ENSO amplitude during positive and negative IPO phases, resulting in the asymmetry of sea surface temperature (SST) anomaly in the tropical Pacific. During positive IPO phases, SSS interdecadal variability contributes positively to El Niño amplitude but negatively to La Niña amplitude by enhancing or reducing SSS interannual variability, and vice versa during negative IPO phases. Quantitatively, the results indicate that the modulation of the ENSO amplitude by the SSS interdecadal variability is -15%–28% during negative IPO phases and -30%–20% during positive IPO phases, respectively. Evidently, the SSS interdecadal variability associated with IPO and its modulation on ENSO amplitude in the tropical Pacific are among factors essentially contributing ENSO diversity.

Keyword: El Niño-Southern Oscillation (ENSO) amplitude; Interdecadal Pacific Oscillation (IPO); ocean salinity variability; tropical Pacific; upper-ocean stratification

1 INTRODUCTION

The tropical Pacific climate system displays interannual-to-interdecadal multi-timescale variabilities, with their synergistic effects, causing extreme weather conditions worldwide (Bjerknes, 1969; Mantua et al., 1997; McPhaden et al., 2006; Ashok and Yamagata, 2009; Ham et al., 2019; Gao et al., 2022). The El Niño-Southern Oscillation (ENSO) is the most prominent signal of interannual variabilities in the tropical Pacific (Rasmusson and Carpenter, 1982). Additionally, ENSO events show pronounced diversity in its spatial and temporal features, which is closely associated with multi-decadal climate variability (Trenberth, 1990; Mantua et al., 1997; Mantua and Hare, 2002; Deser et al., 2004; Rodgers et al., 2004; Feng et al., 2020; Zhang et al., 2022). For example, observations indicated that particularly intense El Niño activities

* Supported by the National Natural Science Foundation of China (No. 42030410) and the Laoshan Laboratory (No. LSKJ202202403). Dr. Rong-Hua ZHANG is additionally supported by the Startup Foundation for Introducing Talent of NUIST
** Corresponding author: rzhang@nuist.edu.cn

are seen during 1980–2000, as marked by the two most extreme El Niño events in 1982 and 1997 (Philander, 1983; Zhang and Levitus, 1997; Zhang et al., 1998, 2022; Santoso et al., 2017). Variations in sea surface temperature (SST) contributing to ENSO diversity reflect the fact that ENSO intensity might be enhanced due to internal variability or external forcing (Abraham et al., 2013; Yeh et al., 2018; Guan et al., 2019; Tokarska et al., 2019; Li et al., 2020; Cai et al., 2021). However, there still exist gaps in understanding of ENSO diversity due to the limitations of the relatively short observational periods.

ENSO diversities in observations are clearly evident on interdecadal timescales in terms of amplitude, zonal position and duration of SST variability (Li et al., 2011; Cai et al., 2018; Freund et al., 2019; Wang et al., 2019). Numerous studies have investigated the related processes and mechanisms, including its interaction dynamics associated with interdecadal variability of ENSO amplitude (Zhang and Levitus, 1997; Choi et al., 2009; Wittenberg, 2009; Li et al., 2011; Ogata et al., 2013; Feng and Tung, 2020; Zhang et al., 2023). It is found that ENSO amplitude varies with the background mean state, which exhibits apparent fluctuations on interdecadal timescales (Rodgers et al., 2004). The pattern of low-frequency fluctuations in the climate system over the Pacific and adjacent regions is characterized by the Interdecadal Pacific Oscillation (IPO) (Power et al., 1999). Traditionally, IPO is considered as a phenomenon in the wider Pacific basin, whose temporal evolution represents interdecadal cycles of positive (warm) and negative (cold) SST anomalies in the Pacific (Mantua et al., 1997; Folland et al., 2002; Mantua and Hare, 2002; Newman et al., 2016). For example, the IPO exhibits negative phases over 1924–1944 and 1977–1998 but positive phases over 1945–1976 and 1999–2014, respectively. Furthermore, the IPO can explain more than half of interdecadal variations of surface air temperature and precipitation over many regions (Dong and Dai, 2015; Power et al., 2021). The frequency and intensity of El Niño events are enhanced during positive IPO phases, while during negative IPO phases it is more favorable for La Niña events to develop (Verdon and Franks, 2006). ENSO properties may be modified by the interactions between ENSO (interannual variability) and background-related interdecadal variabilities (Yeh and Kirtman, 2005; An, 2009; Choi et al., 2012; Dong et al., 2018).

Several studies have explained the complexity of ENSO through various feedbacks that are related to interdecadal variabilities of ocean processes (An and Jin, 2000; Timmermann and Jin, 2002; An, 2009). In addition to the dominant processes causing SST variability, there are other processes that can be responsible for the related ENSO diversities in the tropical Pacific yet, such as the freshwater fluxes at the sea-air interface (Zhang and Busalacchi, 2009; Kang et al., 2017; Gao et al., 2020), the oceanic entrainment at the mixed layer depth in the far western tropical Pacific (Maes et al., 2006; Zheng et al., 2014), and the nonlinear dynamic heating of the heat budget in the tropical Pacific (Jin et al., 2003). These processes can directly or indirectly influence ENSO properties. Similar to temperature, ocean salinity is also an essential variable in determining the thermo-dynamic processes of seawater and ocean circulation. Although ocean salinity is a variable that is not directly involved in atmosphere-ocean interactions, it indirectly affects the upper-ocean temperature by the related ocean physics (Maes et al., 2005; Zhang et al., 2012; Zhi et al., 2019a). Observations and simulations have suggested that ocean salinity influences seawater density and the upper-ocean stratification, which affect the atmosphere-ocean interactions (Fedorov et al., 2004; Huang et al., 2005). Thus, upper-ocean temperature variations are regulated by ocean stratification associated with salinity variability (Zhang et al., 2012). Indeed, several previous studies found that ocean salinity exhibits close relationships with ENSO amplitude (Maes et al., 2005; Zheng et al., 2014; Zhang et al., 2015), Pacific decadal oscillation/interdecadal Pacific oscillation (PDO/IPO) (Lukas, 2001; Zhang et al., 2022; Zhi et al., 2023) and longer-term changes (Skliris et al., 2014, Du et al., 2015; Sathyanarayanan et al., 2021).

Temperature interdecadal variability in the ocean (e.g., SST) and its relationship with the IPO have been studied and established. However, the impacts of salinity interdecadal variability on ENSO, such as the underlying processes and the asymmetric relationship between salinity and ENSO still have considerable uncertainties. At present, relatively short observed datasets cannot cover more than two complete IPO cycles. Realistic model simulations provide long-term data that can be used for analyses. Based on the 110-year ocean salinity simulations from 1901 to 2010, this study aims to reveal the differences in salinity variability associated with the IPO and its modulation on ENSO amplitude during positive and negative IPO phases and the related mechanisms. Therefore, this

study focuses on two issues: one is the spatial distribution of salinity interdecadal variability and its relationship with ENSO amplitude. The other is the ENSO amplitude modulation and the underlying mechanisms associated with salinity interdecadal variability during positive and negative IPO phases.

The remainder of this paper is organized as follows. Section 2 details the data, models, and methods employed in this study. Section 3.1 determines the marked differences in the relationship of sea surface salinity (SSS) with the IPO between negative and positive IPO phases in the tropical Pacific. Section 3.2 investigates the relationship between salinity interdecadal variability and ENSO amplitude during different IPO phases to explain the detailed physical relationships. Section 3.3 studies the asymmetry of cold and warm ENSO events during positive and negative IPO phases associated with SSS interdecadal variability. Section 3.4 explores the possible physical processes responsible for the IPO effects on ENSO by addressing the relationship between SST and SSS variabilities. The main conclusions and discussion of this study are given in Section 4.

2 MODEL, DATA, AND METHOD

2.1 Model and data

In this study, analysis data are produced by the LASG/IAP Climate System Ocean Model (LICOM) developed by the State Key Laboratory of Numerical Modeling for Atmospheric Sciences and Geophysical Fluid Dynamics, Institute of Atmospheric Physics, Chinese Academy of Sciences (Zhang and Liang, 1989; Zeng et al., 1991; Zhang et al., 2020). LICOM version 3 (LICOM3), the latest version of the LICOM, has 360 (longitude) ×218 (latitude) grid points and 30 vertical levels. More detailed configurations of LICOM3 can be found in Lin et al. (2020). In this study, the atmospheric driving dataset for the LICOM3 is the European Center for Medium-Range Weather Forecasts 20th-century reanalysis (Poli et al., 2016), which is used to simulate the monthly mean oceanic fields during 1901–2010. Output variables of monthly mean oceanic data include ocean temperature, ocean salinity, sea surface freshwater flux and salinity budget terms; these data are resampled onto a 1°×1° grid by bilinear interpolation, and their seasonal cycle and trends in response to global warming are removed by band-pass filtering in this study. Then, interdecadal variability is derived from low-pass filtering to remove high-frequency signals for 13 years and shorter, while interannual variability is obtained through high-pass filtering.

2.2 Method

In this study, the mixed layer depth (MLD) and barrier layer thickness (BLT) are used to determine the influences of ocean stratification on SST. The isothermal layer depth (ILD) is calculated as the depth where the temperature is lower than that at 10-m depth, with the temperature change ΔT being defined as 0.2 °C. The MLD is calculated as the depth where the density is larger than that at 10-m depth, with the temperature affecting density change ($\Delta\rho$) being defined to decrease to 0.2 °C (Kara et al., 2000). The BLT is defined as the difference between the MLD and ILD if the MLD is shallower than ILD (Sprintall and Tomczak, 1992; de Boyer Montégut et al., 2004; Bosc et al., 2009).

Moreover, we use the diagnostic method proposed by Zhang et al. (2010) and Zheng and Zhang (2012) to separate the relative contributions of salinity and temperature anomalies to the MLD, BLT, etc. $F(T, S)$ denotes a field that is affected by salinity (S) and temperature (T), which determines ocean density, the MLD and the BLT. $F(T_{\text{inter}}, S_{\text{inter}})$ represents its interannual anomaly that is attributed to temperature and salinity interannual variabilities, $F(T_{\text{clim}}, S_{\text{inter}})$ indicates its interannual variability part that is attributed to salinity interannual variability with climatological temperature being specified; $F(T_{\text{inter}}, S_{\text{clim}})$ denotes its interannual variability part that is attributed to temperature interannual variability contribution with climatological salinity being specified, respectively.

To facilitate direct quantification of climate indices, we define the IPO index as the 13-year running mean of the difference in the annual mean SST anomalies between the tropical central-eastern Pacific (80°E–90°W, 10°S–15°N) and the northern Pacific Ocean (150°E–160° W, 30°N–45°N) (Salzmann and Cherian, 2015). The IPO is highly consistent with the PDO index based on the Empirical Orthogonal Function analysis in terms of temporal evolution and spatial patterns, which implies a reasonable tracking of the low-frequency fluctuations in the Pacific (Huang et al., 2020).

3 RESULT

3.1 Sea surface salinity variability associated with the IPO

To investigate the spatial patterns of SSS

variability at different timescales (Fig.1), its standard deviations in the tropical Pacific from 1901 to 2010 are analyzed based on two signals, i.e., total interannual variability (including interdecadal variability signal, the same below) and interdecadal variability. For the SSS interdecadal variability in the tropical Pacific from 30°S to 30°N, there are large values in the 145°E–175°E region west of the equatorial Pacific, and in the eastern equatorial Pacific close to the American continent and the South Pacific Convergence Zone (Fig.1a). The SSS interdecadal variability presents a "tripolar" mode from the northeast to the southwest in the tropical Pacific. For example, the intensity of the SSS interdecadal variability is the strongest in the western equatorial region, followed by that in the South Pacific, and the weakest east of the Philippines. This conclusion is similar to previous studies (Hu et al., 2020; Shi et al., 2022). Ogata et al. (2013) pointed that the interdecadal variability in the tropical Pacific provides for a background field over which interannual variability can be modulated. The total SSS interannual variability is also relatively larger in the western Pacific compared with the corresponding SSS interdecadal variability. The contribution of the SSS interdecadal variability to the total SSS interannual variability in the western regions is up to 40%–50% (Fig.1b), while in other regions, it is approximately 25%. This result suggests that the SSS interdecadal variability in the tropical Pacific has a strong modulating effect on total SSS interannual variability, which can enhance or reduce total SSS interannual variability.

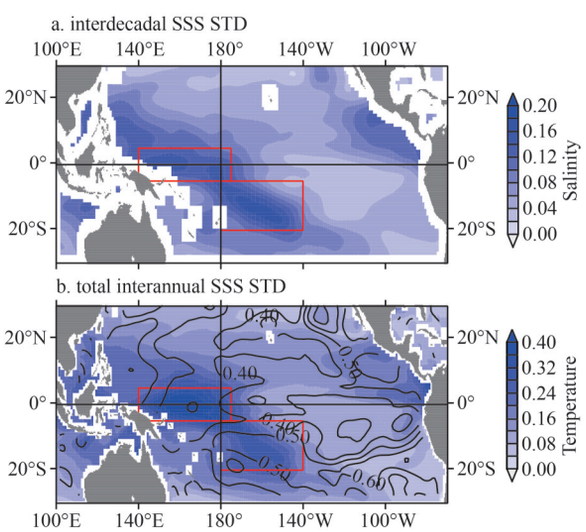

Fig.1 Standard deviation on different scales in the tropical Pacific

a. sea surface salinity (SSS) interdecadal standard deviations (STD); b. total SSS interannual STD. The black contours every 0.1 in (b) present the contribution (%) of SSS interdecadal STD to total SSS interannual STD. The red boxes indicate two key areas for SSS interdecadal variability with stronger intensity and larger contribution to total SSS interannual STD in the tropical Pacific.

Moreover, comparing with the spatial patterns between the total SSS interannual variability and the SSS interdecadal variability, we find that there are slight differences in their locations and intensities in the key areas of the equatorial region and southern Pacific. For example, the SSS interdecadal variability is markedly stronger and has a broader large-value range. Therefore, the region with the largest SSS interdecadal variability (140°E–160°W, 5°S–5°N) is selected for the focused study area and is defined as the key region for the total SSS interannual variability and interdecadal variability in the tropical Pacific.

To determine the relationship of the SSS interdecadal variability with the IPO, we compare the evolution of the SSS interdecadal signal (Fig.2). It can be found that the evolution of the averaged SSS interdecadal variability in the key region shows obvious periodic oscillations on the interdecadal scale. This result is out-of-phase to the temporal evolution of the IPO (R=-0.73), i.e., on the interdecadal scale, negative SSS anomalies correspond to the positive IPO phases, while positive SSS anomalies correspond to the negative IPO phases. Physically, the IPO, being the dominant mode of the SST interdecadal variability in the tropical Pacific, can affect the variability of the

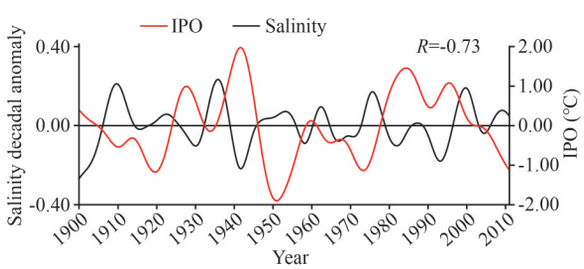

Fig.2 Time series of the IPO index and sea surface salinity (SSS) interdecadal variability averaged in the key box (140°E–160°E, 5°S–5°N) during 1901–2010

The black line denotes the SSS interdecadal variability derived from low-pass filtering to remove high-frequency signals for 13 years, and the red line presents IPO index, the black line is SSS interdecadal variability averaged in the key region, with correlation coefficient being -0.73. The IPO index is defined as the 13-year running mean of the difference in the annual mean SST anomalies between the tropical central-eastern Pacific (80°E–90°W, 10°S–15°N) and the northern Pacific Ocean (150°E–160°W, 30°N–45°N).

related ocean physical fields (Huang et al., 2005), which reflects the strong dynamical links of the warm and cold modes with interdecadal variabilities of ocean physical fields in the central Pacific (Trenberth and Hurrell, 1994; Overland et al., 1999; Nurhati et al., 2011). When IPO, acting as the climate background state, changes in the Pacific, the IPO can correspondingly affect the low-frequency variabilities of the climatic mean state in the Pacific, such as interdecadal variability.

3.2 Relationship of salinity interdecadal variability with the IPO and ENSO amplitude

To clarify the relationship between SSS interdecadal variability and ENSO, we investigate the effect on ENSO intensity due to SSS interdecadal variability related the IPO. Figure 3 presents the evolutions of the Niño3.4 SST index (Niño3.4, the same below), the total SSS interannual variability and its interannual variability part without interdecadal variability effect, which corresponds to the IPO phases in the central-western tropical Pacific; therefore, the contribution of SSS interdecadal variability to the total SSS interannual variability and ENSO amplitude can be demonstrated. As shown in Fig.3a, the evolutions of the Niño3.4, with interdecadal variability effect included or not, exhibit slight differences in its amplitude, while the amplitude of the Niño3.4 presents several differences with interdecadal variability effect included or not. In terms of SSS, the differences in the intensity between the SSS variabilities with and without the interdecadal variability effect can also be found, as shown in Fig.3b. This result indicates that the SSS interdecadal variability in the tropical Pacific can be associated with the IPO in the equatorial Pacific, with the IPO acting as a modulator for interannual variability. This finding is consistent with previous results, i.e., the combined effects of temperature and salinity variability can cause density variation that can reduce or enhance SST interannual variability (Zhang et al., 2022).

The impacts on the SSS interannual variability due to interdecadal variability and ENSO contributions are quantitatively estimated by comparing their absolute differences with interdecadal variability effects being included or not over 1901–2010 (Fig.4). As seen in Fig.4a, the evolutions of the difference between the total interannual Niño3.4 intensity and the total SSS interannual anomalies show great consistency during 1901–2010. It is noted that the temporal evolutions of their difference correspond well to

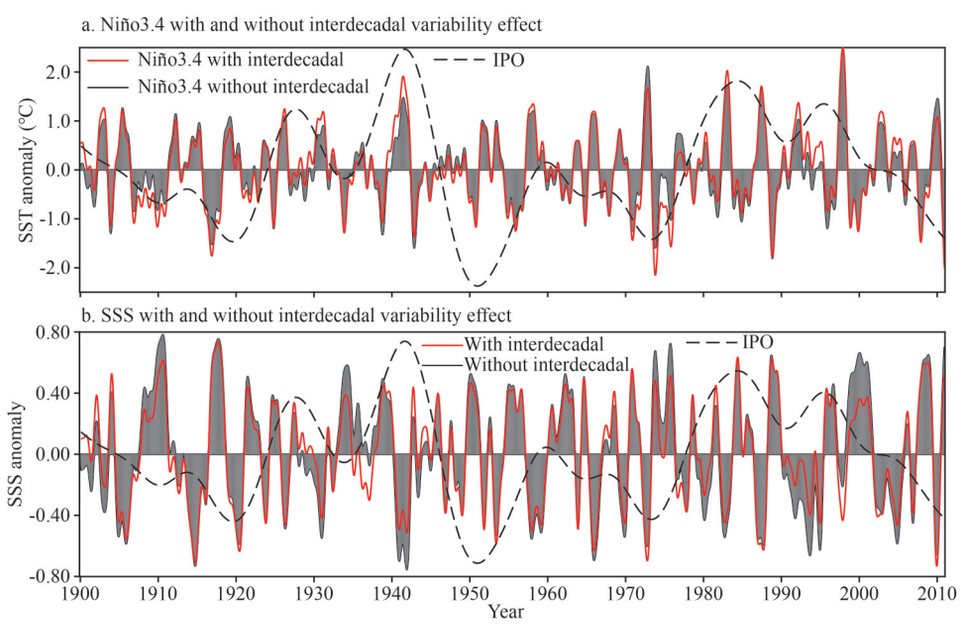

Fig.3 Time series of Niño3.4 sea surface temperature (SST) indexes with and without interdecadal variability (a) and averaged sea surface salinity (SSS) variabilities in the key box with and without interdecadal variability contribution (b)

The red lines and black lines present the variability with and without interdecadal variability of Niño3.4 SST in (a) and that with and without interdecadal variability of SSS in the key area in (b), and the black dot line presents IPO index. In figures, the differences in peaks present the interdecadal variability contribution.

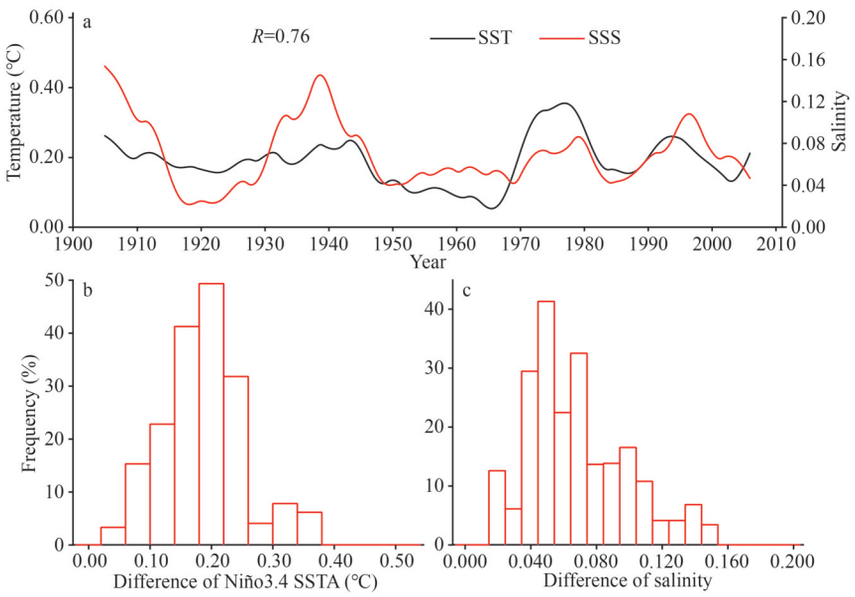

Fig.4 Time series of the absolute difference between total interannual variability and interdecadal variability in Niño3.4 sea surface temperature anomaly (SSTA) and sea surface salinity anomaly (SSSA) in the key box (a); the frequency (%) distribution of the absolute difference between Niño3.4 SST with and without interdecadal variability contribution (b); the frequency (%) distribution of the absolute difference between SSSA with and without interdecadal variability contribution (c)

Red and black lines in (a) present the absolute difference between total interannual variability and interdecadal variability in Niño3.4 SSTA and the absolute difference between total interannual variability and interdecadal variability SSSA in the key box, respectively.

each other, with a correlation coefficient value of 0.76. The significant correlation coefficient implies that ENSO intensity variation is linked to interdecadal variability caused by the total SSS interannual variability during different IPO phases. Thus, it further suggests that ENSO intensity considerably depends on salinity interdecadal variability, i.e., the salinity interdecadal variability can modulate ENSO intensity.

Figure 4b and 4c present the quantitative contributions of the SSS and ENSO interdecadal variabilities to their total interannual variabilities. The difference values between ENSO intensity with and without interdecadal variability contribution range from 0.05 °C to 0.38 °C, and the frequency of the 0.2 °C difference value is the highest (>0.5). The difference values between the SSS with and without interdecadal variability contribution range from 0.02 to 0.16, and the frequency of the 0.05 difference value is the highest (>0.4). The contributions of interdecadal variability to the total interannual variability of the Niño3.4 and SSS anomalies are 23% and 9%, respectively.

Moreover, we use the scatterplot-based regression analysis and examine the corresponding linear relationship between ENSO and SSS variabilities at different timescales to clarify the possible thermodynamic relationship of salinity with the SST. Figure 5 displays the difference in the slopes of the linear regressions between the total SSS interannual anomalies and the Niño3.4 anomalies with and without the interdecadal variability contribution. The results indicate that the difference between the two signals is that one shows interdecadal variability (namely the IPO), while another does not contain the IPO signal. For the total SSS interannual variability without interdecadal variability contribution, the slopes of the linear regressions show that the salinity variability of 1.0 corresponds to the SST anomaly of 1.8 °C, while in terms of the 1.0 salinity variability with interdecadal variability contribution, the corresponding SST anomaly is 1.72 °C, corresponding to the total interannual variability. This phenomenon suggests that the interactions at multiple scales (with and without interdecadal variability contributions) are more complex than those at a single scale (only interannual variability). It implies that the total interannual salinity variability during different IPO phases is related to the interdecadal variabilities effect, with their interactions in the tropical Pacific. These results

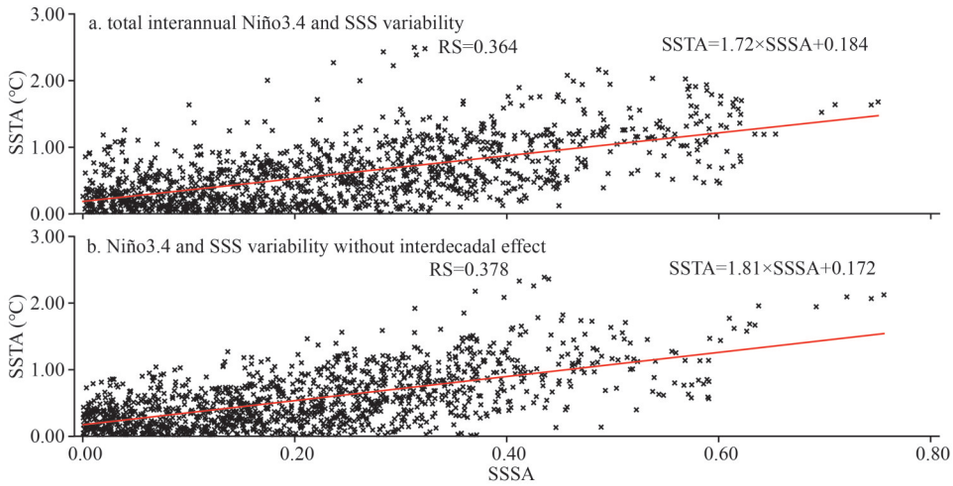

Fig.5 Scatter of monthly absolute Niño3.4 sea surface temperature (SST) index anomaly in response to monthly absolute total interannual SSS anomaly with (a) or without (b) interdecadal variability contribution averaged in the key box (140°E–160°W, 5°S–5°N)

The red lines in (a) and (b) represent SSTA linear regression on SSSA with and without the interdecadal variability.

confirm the conclusion of Okumura et al. (2017), indicating that the interdecadal variation in ENSO amplitude is closely associated with interdecadal variations in background mean state, including salinity field, which can have their positive feedbacks.

Note that the spread does not appear to match the IPO and ENSO phases individually. Therefore, it is important not only to distinguish the differences during negative and positive IPO phases, but also to consider the warm and cold ENSO phases when analyzing the modulating effects on ENSO intensity in the tropical Pacific caused by interdecadal variability.

3.3 Asymmetry of salinity interdecadal variability associated with cold and warm ENSO events during positive and negative IPO phases

This section focuses on classifying warm and cold ENSO events during positive and negative IPO phases during the period of 1901–2010, with detailed analyses for the relationship of ENSO intensity and SSS interdecadal variability during ENSO events for the four different combinations of phases of ENSO and PDO. Here, to avoid spurious effect of interdecadal signal on the selection of ENSO events, the interannual decadal SST variability is moved before selecting ENSO events. In this study, an ENSO event is defined as the event in which interannual SST anomalies are larger (less) than +0.5 °C (-0.5 °C) for 5 consecutive months in the Niño3.4 area. The statistical results show that there were 16 El Niño events and 13 La Niña events during positive IPO phases and 15 El Niño events and 27 La Niña events during negative IPO phases (Table 1). To quantify the relative contribution of salinity interdecadal variability to the selected ENSO events, here, the contribution of interdecadal variability is defined as the difference between the total Niño3.4 interannual variability and the Niño3.4 interannual variability. Figure 6 presents the linear regression coefficients of the contribution of ENSO amplitude to the SSS interdecadal variability during different IPO phases. Compared to the linear regressions for El Niño events during positive and

Table 1 The year with El Niño and La Niña events accompanying with positive and negative IPO phases (1901–2010), respectively

IPO phase	El Niño event (year)	La Niña event (year)
Positive IPO (1900–1904) (1925–1946) (1978–2002)	1900, 1902, 1925, 1930, 1931, 1940, 1941, 1980, 1982, 1986, 1987, 1991, 1993, 1994, 1997, 2002	1903, 1924, 1933, 1938, 1942, 1978, 1981, 1984, 1985, 1988, 1995, 1998, 1999
Negative IPO (1904–1924) (1947–1976) (2003–2010)	1905, 1912, 1914, 1918, 1923, 1951, 1957, 1961, 1963, 1965, 1969, 1972, 2004, 2006, 2009	1906, 1907, 1908, 1909, 1910, 1916, 1917, 1920, 1921, 1922, 1949, 1950, 1954, 1955, 1956, 1962, 1964, 1967, 1970, 1971, 1973, 1974, 1975, 2005, 2007, 2008, 2010

El Niño (La Niña) refer to the years when the Niño3.4 SSTA index during boreal winter (December-January-February, DJF) is greater (less than) than 0.5 °C (-0.5 °C) in amplitude. The DJF Niño3.4 SST index is defined by time series of DJF mean SST anomaly averaged over the Niño3.4 region (170°W–120°W, 5°N–5°S). The seasonal mean anomaly is defined as seasonal mean deviations from a climatological (1901–2010) seasonal mean and a liner trend is removed.

negative IPO phases (Fig.6a & c), the slopes for El Niño events are greater during positive IPO phases than those during negative phases, while the slopes for La Niña events are grater during negative IPO phases than those during positive phases (Fig.6b & d). The relationships of the amplitude variability rates of ENSO events with the SSS interdecadal variability rate exhibit the asymmetry during different IPO phases, namely the dependence on IPO phases. Comparing the linear regressions for El Niño and La Niña events over 1901–2010, it is seen that the El Niño events enhance during positive IPO phases and weaken during positive IPO phases due to the modulation of the SSS interdecadal variability. In contrast, La Niña events weaken during positive IPO phases but strengthen during negative IPO phases, respectively.

Furthermore, the quantitative effect of the SSS interdecadal variability on ENSO intensity can be obtained more clearly (Table 2). For the El Niño events during negative IPO phases, the average SSS interdecadal variability is 0.07, corresponding to

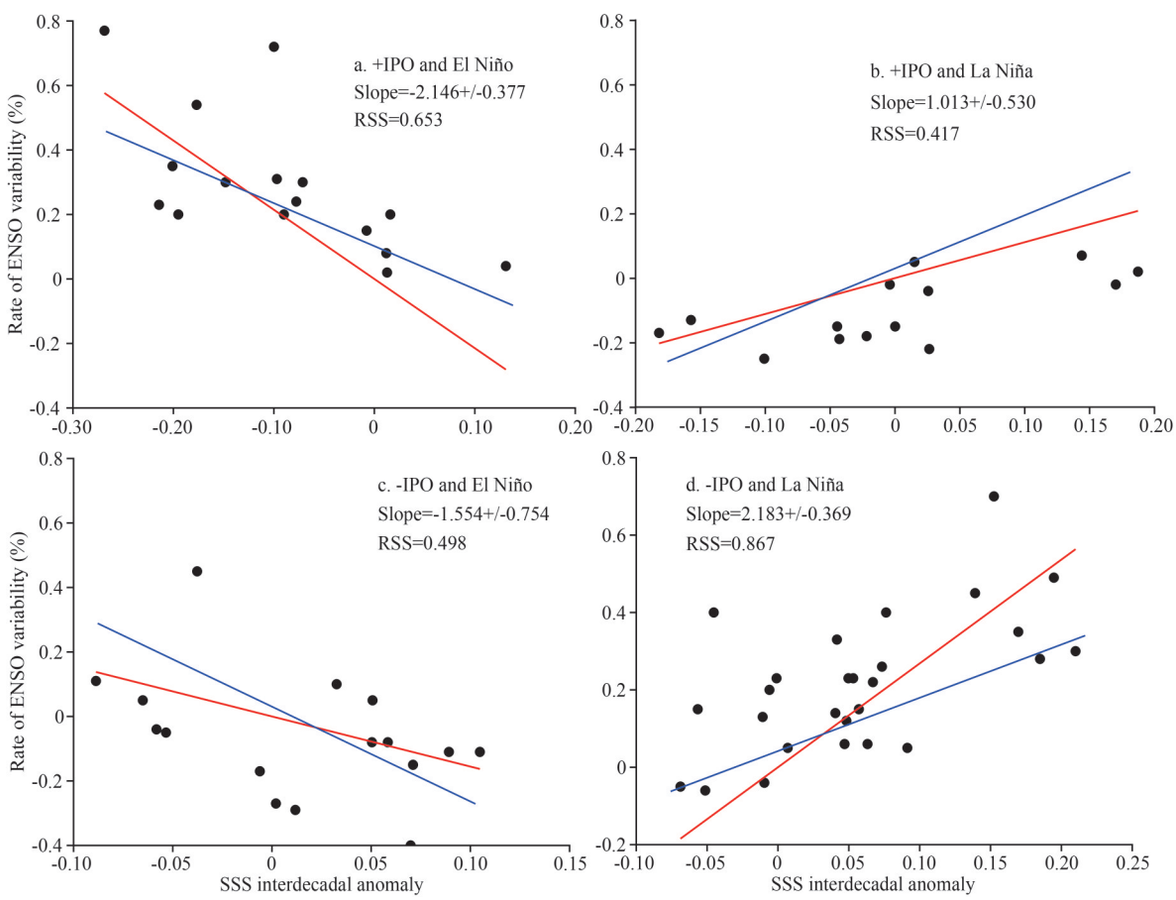

Fig.6 Scatter plots of the change rate of ENSO variability (Niño3.4 without interdecadal/Niño3.4 with interdecadal) and sea surface salinity anomaly (SSSA) interdecadal anomalies averaged in the key box (140°E–160°E, 30°S–30°N) separately illustrated for El Niño events (a) and La Niña events (b) during positive IPO phases, and El Niño events (c) and La Niña events (d) during negative PDO phases

The *x*-axis is the SSS interdecadal variability responding to ENSO events, the *y*-axis is the change rate of ENSO amplitude related interdecadal variability, respectively. Red lines present the linear regression of El Niño and La Niña events during positive and negative IPO phases, the blue lines present the references of all El Niño events or ENSO all La Niña events during 1901–2010.

Table 2 Averaged interdecadal salinity variability and its contribution to ENSO amplitude in the key region during positive and negative IPO phases

Event	Negative IPO		Positive IPO	
	SSS interdecadal anomaly	Contribution to ENSO (%)	SSS interdecadal anomaly	Contribution to ENSO (%)
El Niño	0.07	-15.23	-0.087	20.36
La Niña	0.14	27.50	-0.064	-30.00

-15.23% variability in El Niño intensity. For the El Niño events during positive IPO phases, the averaged SSS interdecadal variability is -0.087, corresponding to a 20.36% contribution of interdecadal variability to La Niña intensity. Conversely, the SSS interdecadal variability for the La Niña events during negative IPO phases is 0.14, with a corresponding contribution of 27.50% to La Niña intensity, while it is -0.064 during positive IPO phases, with a corresponding contribution of -30.00% to La Niña intensity. It demonstrates that since the salinity interdecadal variability is negative during positive IPO phases, it makes a positive contribution to El Niño events and a negative contribution to La Niña events, respectively. On the contrary, the positive salinity interdecadal variability during negative IPO phases exerts a negative contributes to El Niño events and a positive contribution to La Niña events. However, the contribution of the salinity interdecadal variability to El Niño is weak due to the weak salinity interdecadal variability in the key region. For La Niña events, the large salinity interdecadal variability in the key equatorial region has a large contribution to the salinity interdecadal variability during La Niña events.

Generally, total salinity interannual variability exhibits different roles in warm and cold ENSO events due to its differences in contribution to El Niño and La Niña events during negative IPO phases in the key region, which demonstrates that the differences in ENSO intensity between the total interannual variability and interannual variability without interdecadal variability during ENSO events are obviously influenced by the interdecadal variability.

3.4 Possible physical process responsible for IPO effects on ENSO amplitude associated with salinity interdecadal variability

Physically, since the IPO is associated with SSS interdecadal variability in the tropical Pacific, ENSO amplitude displays pronounced interdecadal modulations by the effects on seawater density, which in turn affects the ocean stratification and modulates ENSO intensity (Zhang et al., 2015). As mentioned above, the total SSS interannual variability with the obvious interdecadal signals in the tropical Pacific responds to the IPO signal, which can modulate the SSS interannual variations without interdecadal variability contribution. Previous studies pointed out that the SSS interannual variability can modulate upper-ocean stratification by its effects on MLD and BLT, thereby affecting the upper-ocean temperature (Maes et al., 2005; Zheng and Zhang, 2012; Zhi et al., 2019b).

3.4.1 Relationship between sea surface temperature and salinity

To further clarify the related physical processes responsible for total SST interannual variability associated with the SSS interdecadal variability, we discuss the differences in the spatial patterns between the SSS and the SST anomalies during cold and warm ENSO events for positive and negative IPO phases, respectively. Based on the composite ENSO events, the spatial characteristics of the corresponding total SSS interannual anomalies for ocean stratification are physically identified during warm and cold ENSO events of different IPO phases, as shown in Fig. 7. The results indicate that the total SST and SSS interannual anomalies show noticeable spatial asymmetry. Specifically, during negative IPO phases, the areas with positive SST anomalies in the eastern equatorial Pacific are located farther west, but the intensity of SST variability is weaker than the composite El Niño intensity (Fig.7a). However, negative SST anomalies in the western equatorial Pacific and the eastern and western subtropical regions are higher during positive IPO phases than those during negative IPO phases (Fig.7b). This result indicates that the amplitude of the total SST interannual anomalies related El Niño events in the tropical Pacific decreases during negative IPO phases, resulting in positive SST anomalies in the equatorial and northeastern tropical Pacific, while during positive IPO phases, the total positive SST interannual anomalies appear in the equatorial and southeastern tropical Pacific, with increasing the amplitude of El Niño events.

In terms of La Niña events, the intensity of the total SST interannual anomalies during negative IPO phases is obviously greater than that during positive IPO phases. The total negative SST interannual anomalies for La Niña events during negative IPO phases are found over a large area in the central-eastern, southeastern and northeastern tropical Pacific, with a center being located in the central equatorial Pacific and its western boundary extending to 145°E (Fig.7c), while during IPO positive phases, the westward shift of the range with negative SST anomalies occurs mainly during the La Niña event, the center of negative SST anomalies

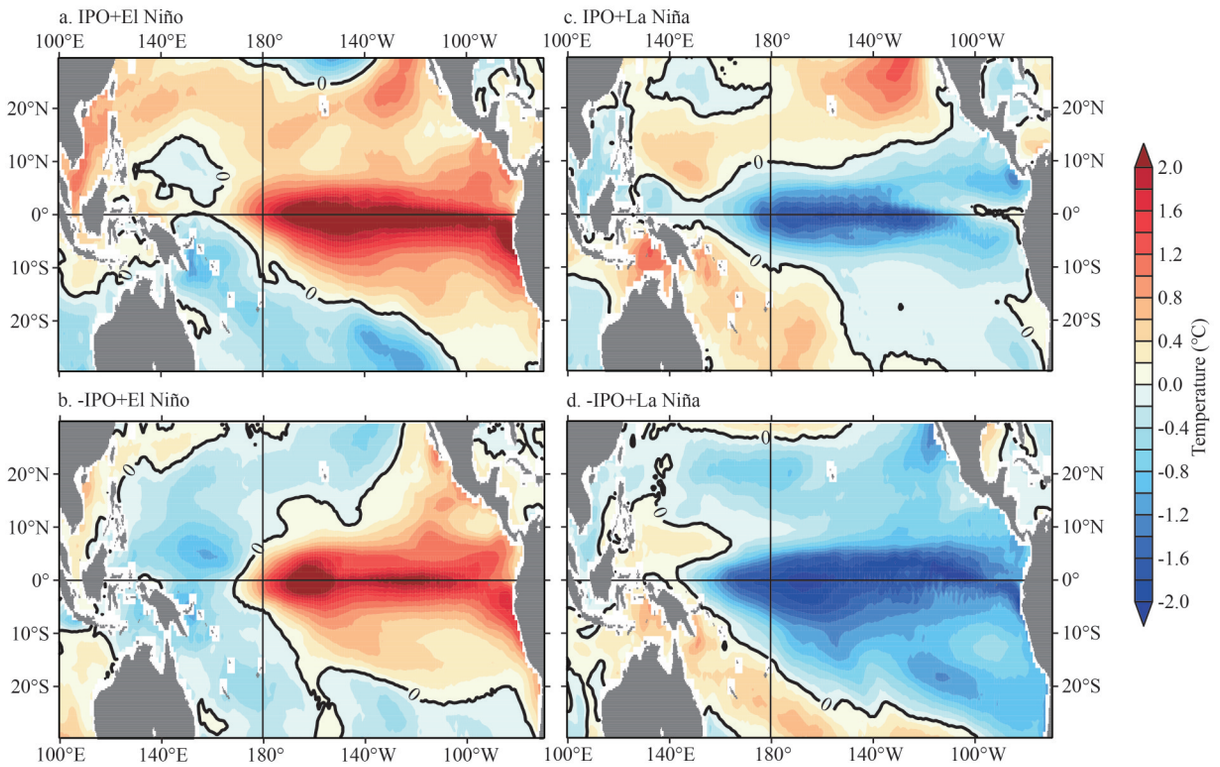

Fig.7 Spatial patterns of composite sea surface temperature (SST) anomalies during ENSO events for the four different combinations of phases of ENSO and PDO for the period 1901–2010 in El Niño (a) and La Niña (c) during positive IPO phases, and El Niño (b) and La Niña (d) during negative IPO phases in the tropical Pacific

ENSO occurrences are sampled using Niño3.4 SST index with 0.5-°C threshold for 5-month mean for defining El Niño and La Niña events, as listed Table 1.

is eastward, and the weaker positive SST anomalies occupy the north and south boundaries of the tropical Pacific (Fig.7d). The results suggest that the region with the total negative SST interannual anomalies in the tropical Pacific extend toward the poles, and the amplitude increases dramatically during negative IPO phases, while the center of negative SST anomalies shrink and move eastward during positive IPO phases.

Note that during positive IPO phases, the intensity of the El Niño events increases as their intensity centers move eastward, while during negative IPO phases, the intensity of the El Niño events weakens with the center moving westward. The differences in the total SST interannual anomalies are mainly found in the southeastern tropical Pacific. Conversely, the intensity of the La Niña events increases with the center moving westward during negative IPO phases but weakens with the center moving eastward during positive IPO phases.

Figure 8 presents the spatial distributions of the total SSS interannual anomalies in cold and warm ENSO events. In terms of El Niño events, a center of the negative SSS anomalies exists in the western equatorial Pacific, and a clear center of positive SSS anomalies appears in the southern tropical Pacific. The intensity center of the negative SSS anomalies during positive IPO phases is stronger than that during negative IPO phases, and the negative SSS anomaly range in the tropical central Pacific expands markedly during positive IPO phases. Moreover, the intensity of the positive SSS anomaly center in the South Pacific is noticeably weaker during positive IPO phases than those during negative IPO phases, which can be reflected in the substantial differences in SSS spatial distribution of El Niño events during positive and negative IPO phases. In addition to the locations of these two centers of SSS anomalies in the Mexican coastal region of the tropical northeastern Pacific, there are also apparent variations. For instance, the range with negative SSS anomalies extends northeastward to the areas west of 120°W and between 10°N and 20°N during negative IPO phases, while the area of negative SSS anomalies is more extensive during positive IPO

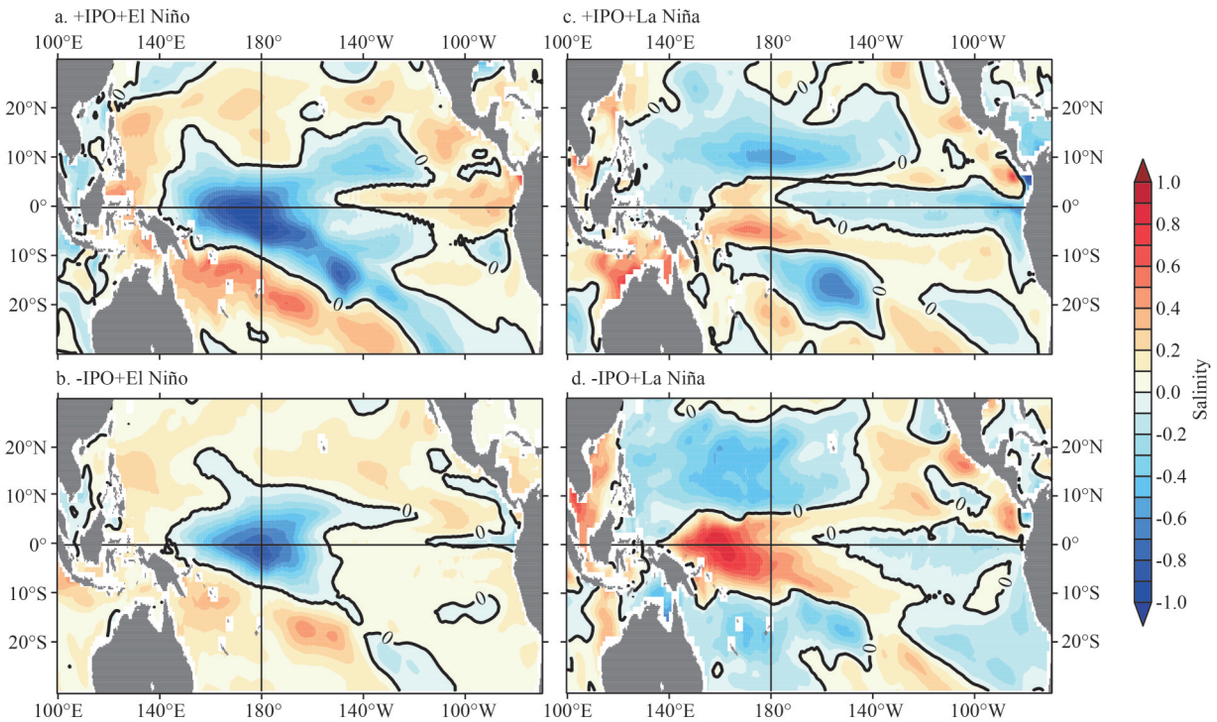

Fig.8 Spatial patterns of composite sea surface salinity (SSS) anomalies during ENSO events for the four different combinations of phases of ENSO and PDO for the period 1901–2010 in El Niño (a) and La Niña (c) during positive IPO phases, and El Niño (b) and La Niña (d) during negative IPO phases in the tropical Pacific

phases, extending northward in the northern tropical Pacific. For La Niña events, a center of positive SSS anomalies occupies the western part of the equatorial region during negative IPO phases. The positive SSS anomalies are more extensive, stronger and more westward in their location during negative IPO phases than those during positive IPO phases. A center of negative SSS anomalies appears in the southern Pacific, which has weaker intensity and a smaller range compared with those during positive IPO phases. The region with positive anomalies in Mexican coastal waters is southward during negative IPO phases but northward during positive IPO phases.

Overall, the differences in ENSO events between positive and negative IPO phases are mainly reflected in the total SSS interannual anomalies in the western part of the equatorial region, which correspond to the weakening or strengthening of the ENSO intensity. For El Niño events, the negative SSS anomalies show differences in intensity and location during different IPO phases, causing the positive SST anomalies to strengthen or weaken, thus contributing to ENSO intensity. In contrast, the positive SSS anomalies also exhibit differences in intensity and position during negative and positive IPO phases during La Niña events, enhancing or weakening the negative SST anomalies, thereby acting to modulate ENSO intensity. These results indicate that in the two key areas the SSS interdecadal variability may play an essential role in the symmetrical modulations on the amplitude of ENSO events.

3.4.2 Physical interpretation

In this study, an essential analysis is achieved to explain the differences in salinity spatial characteristics between cold and warm ENSO events during positive and negative IPO phases by identifying the variations in upper-ocean stratification, the MLD and the BLT. Based on the relationships of the total MLD and BLT interannual anomaly with SST and SSS variabilities, we analyze the dependence of the ocean stratification stability on salinity, i.e., $F(S_{\text{inter}}, T_{\text{inter}}) = F(S_{\text{inter}}) + F(T_{\text{inter}})$. Based on this, the sensitivity of ocean stratification variations to salinity variations is investigated.

Composite El Niño and La Niña related MLD (S_{inter}, T_{clim}) anomalies during positive and negative IPO phases in the tropical Pacific are illustrated in Fig.9. During positive IPO phases, seawater salinity decreases during El Niño events due to negative SSS interannual anomaly contribution, accompanied

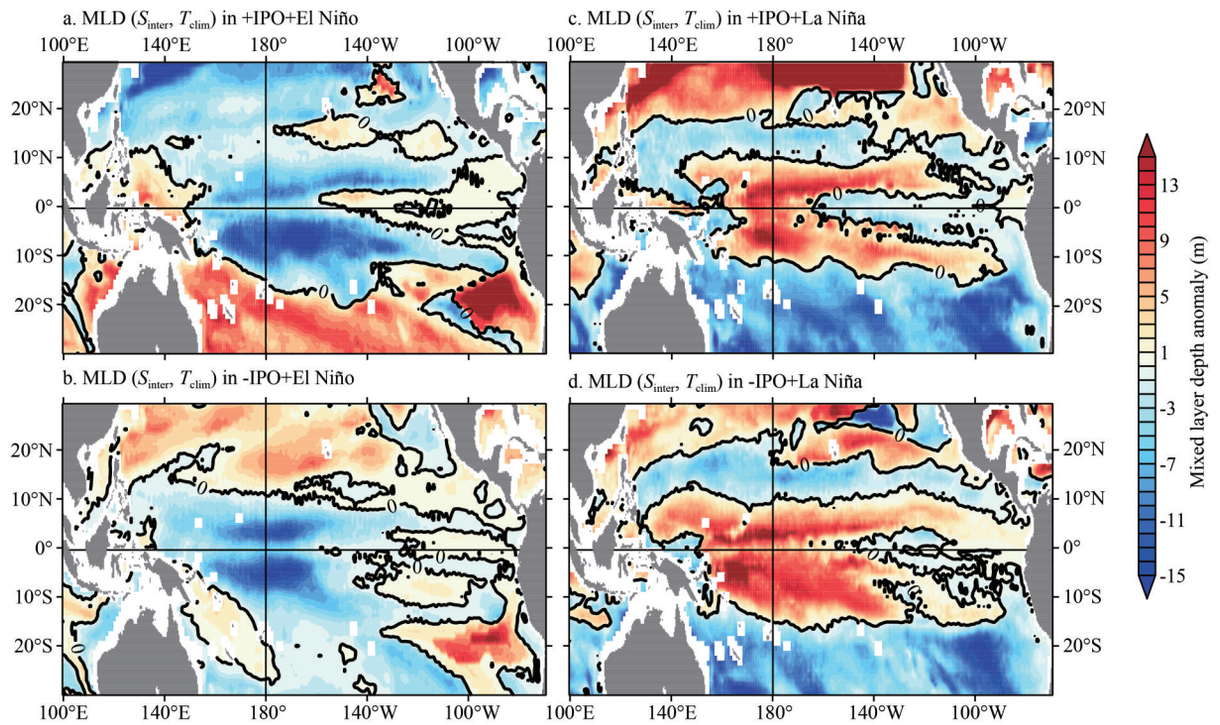

Fig.9 Spatial patterns of composite mixed layer depth (MLD) (S_{inter}, T_{clim}) anomalies during ENSO events for the four different combinations of phases of ENSO and PDO for the period 1901–2010 in El Niño (a) and La Niña (c) during positive IPO phases, and El Niño (b) and La Niña (d) during negative IPO phases in the tropical Pacific

To reveal the role of salinity in MLD, MLD (T_{clim}, S_{inter}) indicates its interannual variability part that is attributed to salinity interannual variability with climatological temperature being specified.

by the negative MLD anomalies in the tropical Pacific. It indicates that the negative SSS anomalies suppress the exchange of upper water with deeper water, leading to an increase in the density gradient at the bottom of the mixed layer and allowing positive BLT anomalies in the western tropical Pacific (Fig.10). In other words, the thicker barrier layer induces the downward transport of heat from the sea surface and stays on the surface layer, leading to a further increase in SST anomalies and contributing to the enhancement of El Niño events. During negative IPO phases on average, there are positive salinity anomalies in the tropical Pacific, which allow positive salinity interdecadal anomalies to be superimposed on El Niño conditions and thus result in weaker negative salinity anomalies and smaller negative MLD anomalies in the western-central Pacific. This situation further reduces the relative BLT near the dateline, making the upper layer of seawater more susceptible to vertical transport and relatively less likely to accumulate surface heat, thereby weakening the intensity of El Niño conditions. The opposite process occurs during positive IPO phases. Specifically, when negative salinity interdecadal anomalies are superimposed on an El Niño event, the negative MLD anomalies increase dramatically, corresponding to an increase in BLT near the dateline. This phenomenon further enhances the SST increase in the central Pacific and strengthens the intensity of El Niño events. For La Niña events, positive MLD anomalies in the tropical Pacific can lead to negative BLT anomalies west of the dateline in the equatorial Pacific. This result indicates that the mixed layer shoaling and barrier thinning make cold salty water upwell through vertical transport, decreasing the SST and promoting the maintenance of La Niña conditions. During negative IPO phases, the positive MLD anomalies in the tropical western Pacific are larger than those during positive IPO phases, and the deeper mixed layer and the thicker barrier layer suppress the upwelling of cold water and enhance the intensity of La Niña conditions.

4 CONCLUSION

Although considerable progress has been made recently in studying climate variability, the internal variability of the climate system limits climate

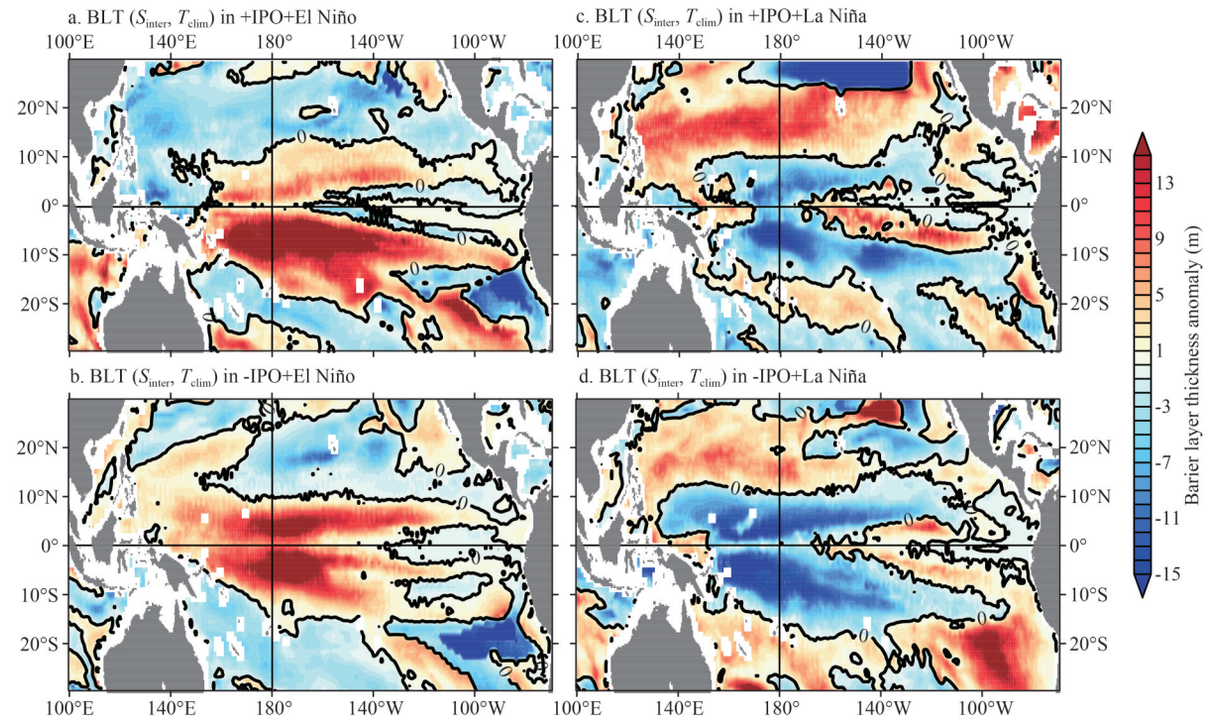

Fig.10 Spatial patterns of composite barrier layer thickness (BLT) (S_{inter}, T_{clim}) anomalies during ENSO events for the four different combinations of phases of ENSO and PDO for the period 1901–2010 in El Niño (a) and La Niña (c) during positive IPO phases, and El Niño (b) and La Niña (d) during negative IPO phases in the tropical Pacific

To reveal the role of salinity in BLT, BLT (T_{clim}, S_{inter}) indicates its interannual variability part that is attributed to salinity interannual variability with climatological temperature being specified.

predictability (Deser et al., 2014). Robustly quantifying internal variability in climate studies remains challenging in explaining ENSO diversity. One of the uncertainties is related to the variabilities at different timescales and the interactions among different physical factors, such as the interactions between IPO and ENSO and between the physical processes associated with salinity variability and ENSO. Due to the limited coverage of SSS observations, no consensus has been achieved as to whether interdecadal variabilities related to IPO in the ENSO amplitude and frequency are entirely driven by noise and independent of the low-frequency variabilities of the mean state, or whether there is an ambiguous relationship. However, based on climate models, the physical processes and their relationships can be investigated. This study focuses on the characteristics of salinity interdecadal variability in the tropical Pacific and its modulations on ENSO, which can contribute to understanding its hitherto elusive causes. The main conclusions are as follows.

The SSS interdecadal variability is different during positive and negative IPO phases, which can lead to differences in the total salinity interannual variability associated with ocean dynamics, resulting in the asymmetry of total SST interannual anomalies. The total salinity interannual variability in the tropical Pacific demonstrates the distinct interdecadal characteristics in the spatio-temporal variations associated with the IPO in the tropical Pacific. Moreover, the salinity interdecadal variability substantially influences the total salinity interannual variability, contributing up to 40%–50% in the tropical Pacific, such as the warm pool and the South Pacific Convergence Zone. Also, the salinity interdecadal variability is highly correlated with the IPO index, i.e., the negative salinity interdecadal anomalies in the equatorial central-western Pacific correspond to the positive IPO phases, and vice versa. Further quantifying the salinity interdecadal variability, we find that using the salinity interdecadal variability as the background field for total SSS interannual variations can indirectly modulate SST variations, and a total SSS interannual variation of 9% (0.08) corresponds to a 23% SST variation (0.19 °C). The characteristics of the salinity interdecadal variability indicate that the multi-scale salinity variations should be fully

considered in investigating climate variabilities, especially in the tropical Pacific.

Since the IPO pattern is a variable of the climate system corresponding to the SSS interdecadal evolution and the positive and negative evolutions of the SSS and SST interannual variabilities in the tropical Pacific, the salinity interdecadal variability as a background field, influences ENSO events by modulating SSS interannual variability. This influence depends on the phases between ENSO and IPO. During positive IPO phases, negative salinity interdecadal variability positively enhances El Niño events and negatively suppresses La Niña events. The amplitude of the SSS interdecadal variation varies slightly, and the influence of the SSS interdecadal variability on ENSO events is inconsistent in their contribution to La Niña and El Niño events (about from -30.0% to 20.0%). During negative IPO phases, the SSS interdecadal variability shows a positive contribution when the SSS interdecadal variability is negative. However, the SSS interdecadal variability in the equatorial key region is weak, and its interdecadal contribution to El Niño events is also small, with a contribution of -15.0%. In terms of La Niña events, the SSS interdecadal variability is prominent in the equatorial key region, with a contribution of 27.0%.

Physically, the total salinity interannual variability in the tropical Pacific is regulated by SSS interdecadal variability, which in turn modulates SST interannual variability by affecting ocean stratification. During positive IPO phases, since the negative salinity anomalies in the western and central Pacific, the negative MLD anomalies become larger, and the vertical transport of the upper seawater becomes weaker. In this situation, the surface heat is relatively easy to accumulate, and thus the intensity of El Niño events increases. During negative IPO phases, the positive MLD anomalies in the tropical western and central Pacific are larger than that during positive IPO phases, indicating a deeper mixed layer and a shallower barrier layer. Such mixed and barrier layers allow the upwelling of cold water, aggravating La Niña events and increasing their duration accordingly Fig.11.

5 DISCUSSION

The modulations of ENSO by interdecadal variability have received enormous attention (An and Wang, 2000; Zheng and Zhang, 2012; Zhang et al., 2015). The ENSO is expected to be modulated on interdecadal scales, particularly when the tropical climate background state (such as the IPO) fluctuates strongly (An, 2018). The combined analyses suggest that the modulation of the teleconnection of ENSO by the IPO varies with both IPO phases and ENSO events because the modulation patterns are neither symmetrically opposite between warm and cold IPO phases, nor between El Niño and La Niña events (Dong et al., 2018). A set of numerical experiments forced by different combinations of the IPO- and ENSO-related SST fields further illustrates the asymmetric modulation effect of the IPO, which depends primarily on the background state and the SST anomalies in the tropical Pacific, and secondarily on extratropical SST anomalies (Imada and Kimoto, 2009; Lin et al., 2018).

Based on the results of 100 years of on-line simulation, this paper focuses on the modulation

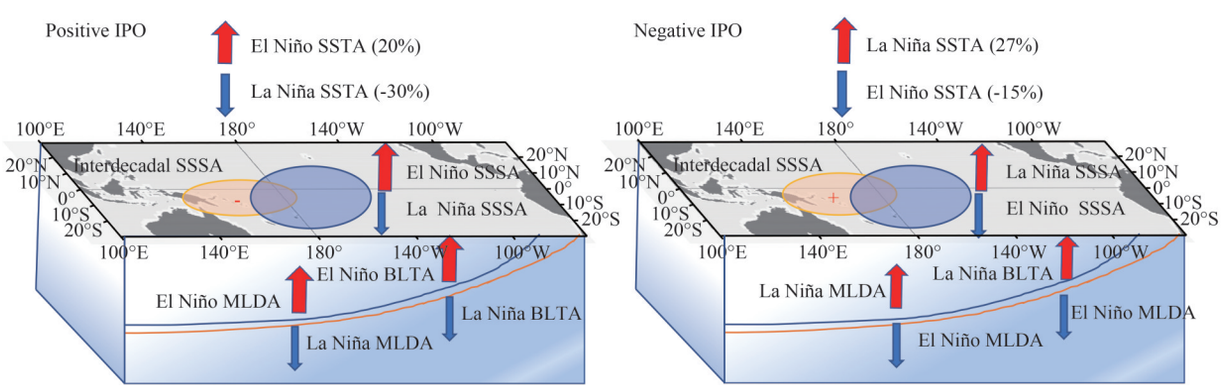

Fig.11 A schematic illustration of salinity anomalies and the related physics during positive and negative IPO phases

The total salinity interannual anomaly originates from interdecadal salinity during IPO phases, leading to enhanced/reduced total interannual salinity variability in the tropical Pacific, then, inducing the modulation on SSTA, ENSO amplitude by altering upper-ocean stratification, as illustrated in the figure. The red arrows indicate a case in which an anomaly is increased. And the blue arrows indicate a case in which an anomaly is reduced.

effect of interdecadal salinity changes associated with IPO on ENSO intensity from the perspective of salinity effect. The relationship between the different scales can be explained physically, which is consistent with our current understanding that salinity affects sea surface temperature. It is well known that the interrelationship of climate changes at different scales in the climate system is very complex, not only with one-way effects, but also with mutual effects. For example, for IPO and ENSO, two important modes in the Pacific Ocean, not only have found the impact of IPO on the diversity of ENSO (Choi et al., 2012), but also the impact of ENSO on IPO (Yeh et al., 2005). Even they interact at the same time (Rodgers et al., 2004). In this paper, the interdecadal variation of the tropical Pacific is taken as the background field to analyze its influence on the interannual variation. This relationship is discussed in the previous research in the introduction, but there are certain defects in the analysis of this relationship by using the observation and simulation results. The IPO can cause salinity variations, as well as other variability in the coupled ocean-atmosphere system, so it may not be justified to argue that the ENSO variability during different phases of the IPO is all due to salinity. Therefore, the causal relationship proposed in this study may not be very robust. A series of experiments, such as model sensitivity experiments, are needed to further verify the relationship between decadal and interannual changes, especially, the process and causality of salinity response to multi-scale changes.

Climate variability is a popular topic in the science community because of its potential impact on society. The primary focus of this study is on investigating the relationship between ENSO diversity and ocean variability (such as SST and IPO) on different timescales. However, this study remains many open questions because ENSO diversity is a quite complex issue that not only involves multi-scale impacts (such as the influences of global warming), but also is influenced by the multi-physical processes of the atmosphere and ocean, such as ocean thermocline feedback. Currently, identifying the impacts of SSS interdecadal variability on ENSO amplitude during IPO phases helps to explain why the interdecadal modulation of ENSO amplitude has been prevalent over the past decade. Since ENSO is the dominant mode of interannual variability, its amplitude modulation has significant implications for the occurrence of global climate extremes.

6 DATA AVAILABILITY STATEMENT

All simulation data generated by the LASG/IAP Climate System Ocean Model (LICOM) developed by ocean group of Institute of Atmospheric Physics, Chinese Academy of Sciences (LIN Pengfei, LIU Hailong et al.).

7 ACKNOWLEDGMENT

The authors also wish to thank the computer resources from Earthlab in IAP.

References

Abraham J P, Baringer M, Bindoff N L et al. 2013. A review of global ocean temperature observations: implications for ocean heat content estimates and climate change. *Reviews of Geophysics*, **51**(3): 450-483, https://doi.org/10.1002/rog.20022.

An S-I. 2018. Impact of pacific decadal oscillation on frequency asymmetry of El Niño and La Niña events. *Advances in Atmospheric Sciences*, **35**(05): 493-494, https://doi.org/10.1007/s00376-018-8024-7.

An S-I, Wang B. 2000. Interdecadal change of the structure of the ENSO mode and its impact on the ENSO frequency. *Journal of Climate*, **13**: 2044-2055, https://doi.org/10.1175/1520-0442(2000)013<2044:ICOTSO>2.0.CO;2.

An S-I, Jin F F. 2000. An Eigen analysis of the interdecadal changes in the structure and frequency of ENSO mode. *Geophysical Research Letters*, **27**(16): 2573-2576, https://doi.org/10.1029/1999GL011090.

An S-I. 2009. A review of interdecadal changes in the nonlinearity of the El Niño-Southern Oscillation. *Theoretical and Applied Climatology*, **97**(1): 29-40, https://doi.org/10.1007/s00704-008-0071-z.

Ashok K, Yamagata T. 2009. The El Niño with a difference. *Nature*, **461**(7263): 481-484, https://doi.org/10.1038/461481a.

Bjerknes J. 1969. Atmospheric teleconnections from the equatorial Pacific. *Monthly Weather Review*, **97**(3): 163-172, https://doi.org/10.1175/1520-0493(1969)097<0163:ATFTEP>2.3.CO;2.

Bosc C, Delcroix T, Maes C. 2009. Barrier layer variability in the western Pacific warm pool from 2000 to 2007. *Journal of Geophysical Research*: *Oceans*, **114**(C6): C06023, https://doi.org/10.1029/2008JC005187.

Cai W J, Santoso A, Collins M et al. 2021. Changing El Niño-Southern Oscillation in a warming climate. *Nature Reviews Earth & Environment*, **2**(9): 628-644, https://doi.org/10.1038/s43017-021-00199-z.

Cai W J, Wang G J, Dewitte B et al. 2018. Increased variability of eastern Pacific El Niño under greenhouse warming. *Nature*, **564**(7735): 201-206, https://doi.org/10.1038/s41586-018-0776-9.

Choi J, An S I, Dewitte B et al. 2009. Interactive feedback between the tropical Pacific decadal oscillation and ENSO in a coupled general circulation model. *Journal of Climate*, **22**(24): 6597-6611, https://doi.org/10.1175/2009JCLI2782.1.

Choi J, An S I, Yeh S W. 2012. Decadal amplitude modulation of two types of ENSO and its relationship with the mean state. *Climate Dynamics*, **38**(11-12): 2631-2644, https://doi.org/10.1007/s00382-011-1186-y.

de Boyer Montégut C, Madec G, Fischer A S et al. 2004. Mixed layer depth over the global ocean: an examination of profile data and a profile-based climatology. *Journal of Geophysical Research*: *Oceans*, **109**(C12): C12003, https://doi.org/10.1029/2004JC002378.

Delcroix T, Cravatte S, McPhaden M J. 2007. Decadal variations and trends in tropical pacific sea surface salinity since 1970. *Journal of Geophysical Research*: *Oceans*, **112**(C3): C03012, https://doi.org/10.1029/2006JC003801.

Deser C, Phillips A S, Alexander M A et al. 2014. Projecting North American climate over the next 50 years: uncertainty due to internal variability. *Journal of Climate*, **27**(6): 2271-2296, https://doi.org/10.1175/JCLI-D-13-00451.1.

Deser C, Phillips A S, Hurrell J W. 2004. Pacific interdecadal climate variability: linkages between the tropics and the north Pacific during boreal winter since 1900. *Journal of Climate*, **17**(16): 3109-3124, https://doi.org/10.1175/1520-0442(2004)017<3109:PICVLB>2.0.CO;2.

Dong B, Dai A G. 2015. The influence of the interdecadal pacific oscillation on temperature and precipitation over the globe. *Climate Dynamics*, **45**(9-10): 2667-2681, https://doi.org/10.1007/s00382-015-2500-x.

Dong B, Dai A G, Vuille M et al. 2018. Asymmetric modulation of ENSO teleconnections by the interdecadal pacific oscillation. *Journal of Climate*, **31**(18): 7337-7361, https://doi.org/10.1175/JCLI-D-17-0663.1.

Du Y, Zhang Y H, Feng M et al. 2015. Decadal trends of the upper ocean salinity in the tropical Indo-Pacific since mid-1990s. *Scientific Reports*, **5**: 16050, https://doi.org/10.1038/srep16050.

Fedorov A V, Pacanowski R C, Philander S G et al. 2004. The effect of salinity on the wind-driven circulation and the thermal structure of the upper ocean. *Journal of Physical Oceanography*, **34**(9): 1949-1966, https://doi.org/10.1175/1520-0485(2004)034<1949:TEO- SOT>2.0.CO;2.

Feng Y, Chen X Y, Tung K K. 2020. ENSO diversity and the recent appearance of Central Pacific ENSO. *Climate Dynamics*, **54**(1-2): 413-433, https://doi.org/10.1007/s00382-019-05005-7.

Feng Y, Tung K K. 2020. ENSO modulation: real and apparent; implications for decadal prediction. *Climate Dynamics*, **54**(1-2): 615-629, https://doi.org/10.1007/s00382-019-05016-4.

Folland C K, Renwick J A, Salinger M J et al. 2002. Relative influences of the interdecadal pacific oscillation and ENSO on the South Pacific convergence zone. *Geophysical Research Letters*, **29**(13): 1643, https://doi.org/10.1029/2001GL014201.

Freund M B, Henley B J, Karoly D J et al. 2019. Higher frequency of Central Pacific El Niño events in recent decades relative to past centuries. *Nature Geoscience*, **12**(6): 450-455, https://doi.org/10.1038/s41561-019-0353-3.

Gao C, Chen M N, Zhou L et al. 2022. The 2020-21 prolonged La Niña evolution in the tropical Pacific. *Science China Earth Sciences*, **65**(12): 2248-2266, https://doi.org/10.1007/s11430-022-9985-4.

Gao C, Zhang R-H, Karnauskas K B et al. 2020. Separating freshwater flux effects on ENSO in a hybrid coupled model of the tropical Pacific. *Climate Dynamics*, **54**(11-12): 4605-4626, https://doi.org/10.1007/s00382-020-05245-y.

Guan C, McPhaden M J, Wang F et al. 2019. Quantifying the role of oceanic feedbacks on ENSO asymmetry. *Geophysical Research Letters*, **46**(4): 2140-2148, https://doi.org/10.1029/2018gl081332.

Ham Y G, Kim J H, Luo J J. 2019. Deep learning for multi-year ENSO forecasts. *Nature*, **573**(7775): 568-572, https://doi.org/10.1038/s41586-019-1559-7.

Hu S J, Sprintall J, Guan C et al. 2020. Observed triple mode of salinity variability in the thermocline of tropical Pacific Ocean. *Journal of Geophysical Research*: *Oceans*, **125**(9): e2020JC016210, https://doi.org/10.1029/2020JC016210.

Huang B Y, Mehta V M, Schneider N. 2005. Oceanic response to idealized net atmospheric freshwater in the Pacific at the decadal time scale. *Journal of Physical Oceanography*, **35**(12): 2467-2486, https://doi.org/10.1175/JPO2820.1.

Huang X, Zhou T J, Dai A G et al. 2020. South Asian summer monsoon projections constrained by the interdecadal Pacific oscillation. *Science Advances*, **6**(11): eaay6546, https://doi.org/10.1126/sciadv.aay6546.

Imada Y, Kimoto M. 2009. ENSO amplitude modulation related to Pacific decadal variability. *Geophysical Research Letters*, **36**(3): L03706, https://doi.org/10.1029/2008GL036421.

Jin F F, An S I, Timmermann A et al. 2003. Strong El Niño events and nonlinear dynamical heating. *Geophysical Research Letters*, **30**(3): 1120, https://doi.org/10.1029/2002GL016356.

Kang X B, Zhang R H, Wang G S. 2017. Effects of different freshwater flux representations in an ocean general circulation model of the tropical Pacific. *Science Bulletin*, **62**(5): 345-351, https://doi.org/10.1016/j.scib.2017.02.002.

Kara A B, Rochford P A, Hurlburt H E. 2000. An optimal definition for ocean mixed layer depth. *Journal of Geophysical Research*: *Oceans*, **105**(C7): 16803-16821, https://doi.org/10.1029/2000JC900072.

Li G C, Cheng L J, Zhu J et al. 2020. Increasing ocean stratification over the past half-century. *Nature Climate*

Change, **10**(12): 1116-1123, https://doi.org/10.1038/s41558-020-00918-2.

Li J B, Xie S P, Cook E R et al. 2011. Interdecadal modulation of El Niño amplitude during the past millennium. *Nature Climate Change*, **1**(2): 114-118, https://doi.org/10.1038/nclimate1086.

Lin P F, Yu Z P, Liu H L et al. 2020. LICOM model datasets for the CMIP6 ocean model intercomparison project. *Advances in Atmospheric Sciences*, **37**(3): 239-249, https://doi.org/10.1007/s00376-019-9208-5.

Lin R P, Zheng F, Dong X. 2018. ENSO frequency asymmetry and the Pacific decadal oscillation in observations and 19 CMIP5 models. *Advances in Atmospheric Sciences*, **35**(5): 495-506, https://doi.org/10.1007/s00376-017-7133-z.

Lukas R. 2001. Freshening of the upper thermocline in the north pacific subtropical gyre associated with decadal changes of rainfall. *Geophysical Research Letters*, **28**(18): 3485-3488, https://doi.org/10.1029/2001GL013116.

Maes C, Ando K, Delcroix T et al. 2006. Observed correlation of surface salinity, temperature and barrier layer at the eastern edge of the western Pacific warm pool. *Geophysical Research Letters*, **33**(6): L06601, https://doi.org/10.1029/2005GL024772.

Maes C, Picaut J, Belamari S. 2005. Importance of the salinity barrier layer for the buildup of El Niño. *Journal of Climate*, **18**(1): 104-118, https://doi.org/10.1175/JCLI-3214.1.

Mantua N J, Hare S R, Zhang Y et al. 1997. A Pacific interdecadal climate oscillation with impacts on salmon production. *Bulletin of the American Meteorological Society*, **78**(6): 1069-1080, https://doi.org/10.1175/1520-0477(1997)078<1069:APICOW>2.0.CO;2.

Mantua N J, Hare S R. 2002. The Pacific decadal oscillation. *Journal of Oceanography*, **58**(1): 35-44, https://doi.org/10.1023/A:1015820616384.

McPhaden M J, Zebiak S E, Glantz M H. 2006. ENSO as an integrating concept in earth science. *Science*, **314**(5806): 1740-1745, https://doi.org/10.1126/science.1132588.

Newman M, Alexander M A, Ault T R et al. 2016. The Pacific decadal oscillation, revisited. *Journal of Climate*, **29**(12): 4399-4427, https://doi.org/10.1175/JCLI-D-15-0508.1.

Nurhati I S, Cobb K M, Di Lorenzo E. 2011. Decadal-scale SST and salinity variations in the central tropical Pacific: signatures of natural and anthropogenic climate change. *Journal of Climate*, **24**(13): 3294-3308, https://doi.org/10.1175/2011JCLI3852.1.

Ogata T, Xie S P, Wittenberg A et al. 2013. Interdecadal amplitude modulation of El Niño-Southern Oscillation and its impact on tropical pacific decadal variability. *Journal of Climate*, **26**(18): 7280-7297, https://doi.org/10.1175/JCLI-D-12-00415.1.

Okumura Y M, Sun T Y, Wu X. 2017. Asymmetric modulation of El Niño and La Niña and the linkage to tropical Pacific decadal variability. *Journal of Climate*, **30**(12): 4705-4733, https://doi.org/10.1175/JCLI-D-16-0680.1.

Overland J E, Salo S, Adams J M. 1999. Salinity signature of the Pacific decadal oscillation. *Geophysical Research Letters*, **26**(9): 1337-1340, https://doi.org/10.1029/1999GL900241.

Philander S G H. 1983. Meteorology: anomalous El Niño of 1982-83. *Nature*, **305**(5029): 16, https://doi.org/10.1038/305016a0.

Poli P, Hersbach H, Dee D P et al. 2016. ERA-20C: an atmospheric reanalysis of the twentieth century. *Journal of Climate*, **29**(11): 4083-4097, https://doi.org/10.1175/JCLI-D-15-0556.1.

Power S, Casey T, Folland C et al. 1999. Inter-decadal modulation of the impact of ENSO on Australia. *Climate Dynamics*, **15**(5): 319-324, https://doi.org/10.1007/s003820050284.

Power S, Lengaigne M, Capotondi A et al. 2021. Decadal climate variability in the tropical pacific: characteristics, causes, predictability, and prospects. *Science*, **374**(6563): eaay9165, https://doi.org/10.1126/science.aay9165.

Rasmusson E M, Carpenter T H. 1982. Variations in tropical sea surface temperature and surface wind fields associated with the Southern Oscillation/El Niño. *Monthly Weather Review*, **110**(5): 354-384, https://doi.org/10.1175/1520-0493(1982)110<0354:VITSST>2.0.CO;2.

Rodgers K B, Aumont O, Madec G et al. 2004. Radiocarbon as a thermocline proxy for the eastern equatorial Pacific. *Geophysical Research Letters*, **31**(14): L14314, https://doi.org/10.1029/2004GL019764.

Salzmann M, Cherian R. 2015. On the enhancement of the Indian summer monsoon drying by Pacific multidecadal variability during the latter half of the twentieth century. *Journal of Geophysical Research*: *Atmosphere*, **120**: 9103-9118, https://doi.org/10.1002/2015JD023313.

Santoso A, Mcphaden M J, Cai W J. 2017. The defining characteristics of ENSO extremes and the strong 2015/2016 El Niño. *Reviews of Geophysics*, **55**(4): 1079-1129, https://doi.org/10.1002/2017RG000560.

Sathyanarayanan A, Köhl A, Stammer D. 2021. Ocean salinity changes in the global ocean under global warming conditions. Part I: mechanisms in a strong warming scenario. *Journal of Climate*, **34**(20): 8219-8236, https://doi.org/10.1175/JCLI-D-20-0865.1.

Shi H Y, Du L, Ni X B. 2022. Salinity variability modes in the Pacific Ocean from the perspectives of the Interdecadal Pacific Oscillation and global warming. *Journal of Geophysical Research*: *Oceans*, **127**(7): e2021JC018092, https://doi.org/10.1029/2021JC018092.

Skliris N, Marsh R, Josey S A et al. 2014. Salinity changes in the World Ocean since 1950 in relation to changing surface freshwater fluxes. *Climate Dynamics*, **43**(3): 709-736, https://doi.org/10.1007/s00382-014-2131-7.

Sprintall J, Tomczak M. 1992. Evidence of the barrier layer in the surface layer of the tropics. *Journal of Geophysical Research*: *Oceans*, **97**(C5): 7305-7316, https://doi.org/10.1029/92JC00407.

Timmermann A, Jin F F. 2002. A nonlinear mechanism for decadal El Niño amplitude changes. *Geophysical*

Research Letters, **29**(1): 1003, https://doi.org/10.1029/2001GL013369.

Tokarska K B, Hegerl G C, Schurer A P et al. 2019. Quantifying human contributions to past and future ocean warming and thermosteric sea level rise. *Environmental Research Letters*, **14**(7): 074020, https://doi.org/10.1088/1748-9326/ab23c1.

Trenberth K E. 1990. Recent observed interdecadal climate changes in the Northern Hemisphere. *Bulletin of the American Meteorological Society*, **71**(7): 988-993, https://doi.org/10.1175/1520-0477(1990)071<0988:roicci>2.0.co;2.

Trenberth K E, Hurrell J W. 1994. Decadal atmosphere-ocean variations in the Pacific. *Climate Dynamics*, **9**(6): 303-319, https://doi.org/10.1007/BF00204745.

Verdon D C, Franks S W. 2006. Long-term behaviour of ENSO: interactions with the PDO over the past 400 years inferred from paleoclimate records. *Geophysical Research Letters*, **33**(6): L06712, https://doi.org/10.1029/2005GL025052.

Wang B, Luo X, Yang Y M et al. 2019. Historical change of El Niño properties sheds light on future changes of extreme El Niño. *Proceedings of the National Academy of Sciences of the United States of America*, **116**(45): 22512-22517, https://doi.org/10.1073/pnas.1911130116.

Weisberg R H, Wang C Z. 1997. A western Pacific oscillator paradigm for the El Niño-Southern oscillation. *Geophysical Research Letters*, **24**(7): 779-782, https://doi.org/10.1029/97GL00689.

Wittenberg A T. 2009. Are historical records sufficient to constrain ENSO simulations? *Geophysical Research Letters*, **36**(12): L12702, https://doi.org/10.1029/2009GL038710.

Yeh S W, Cai W J, Min S K et al. 2018. ENSO atmospheric teleconnections and their response to greenhouse gas forcing. *Reviews of Geophysics*, **56**(1): 185-206, https://doi.org/10.1002/2017RG000568.

Yeh S W, Kirtman B P. 2005. Pacific decadal variability and decadal ENSO amplitude modulation. *Geophysical Research Letters*, **32**(5): L05703, https://doi.org/10.1029/2004GL021731.

Zeng Q C, Zhang X H, Zhang R-H. 1991. A design of an oceanic GCM without the rigid lid approximation and its application to the numerical simulation of the circulation of the Pacific Ocean. *Journal of Marine Systems*, **1**(3): 271-292, https://doi.org/10.1016/0924-7963(91)90033-Q.

Zhang R-H, Busalacchi A J. 2009. Freshwater flux (FWF)-induced oceanic feedback in a hybrid coupled model of the tropical Pacific. *Journal of Climate*, **22**(4): 853-879, https://doi.org/10.1175/2008JCLI2543.1.

Zhang R-H, Gao C, Feng L C. 2022. Recent ENSO evolution and its real-time prediction challenges. *National Science Review*, **9**(4): nwac052, https://doi.org/10.1093/nsr/nwac052.

Zhang R-H, Gao C, Kang X B et al. 2015. ENSO modulations due to interannual variability of freshwater forcing and ocean biology-induced heating in the tropical Pacific. *Scientific Reports*, **5**(1): 18506, https://doi.org/10.1038/srep18506.

Zhang R-H, Rothstein L M, Busalacchi A J. 1998. Origin of upper-ocean warming and El Niño change on decadal scales in the tropical Pacific Ocean. *Nature*, **39**(6670): 879-883, https://doi.org/10.1038/36081.

Zhang R-H, Levitus S. 1997. Structure and cycle of decadal variability of upper ocean temperature in the North Pacific. *Journal of. Climate*, **10**: 710-727, https://doi.org/10.1175/1520-0442(1997)0102.0.CO;2.

Zhang R-H, Wang G, Chen D K et al. 2010. Interannual biases induced by freshwater flux and coupled feedback in the tropical Pacific. *Monthly Weather Review*, **138**(5): 1715-1737, https://doi.org/10.1175/2009mwr3054.1.

Zhang R-H, Yu Y Q, Song Z Y et al. 2020. A review of progress in coupled ocean-atmosphere model developments for ENSO studies in China. *Journal of Oceanology and Limnology*, **38**(4): 930-961, https://doi.org/10.1007/s00343-020-0157-8.

Zhang R-H, Zheng F, Zhu J S et al. 2012. Modulation of El Niño-Southern Oscillation by freshwater flux and salinity variability in the tropical Pacific. *Advances in Atmospheric Sciences*, **29**(4): 647-660, https://doi.org/10.1007/s00376-012-1235-4.

Zhang R-H, Zhou G H, Zhi H et al. 2023. Salinity interdecadal variability in the western equatorial Pacific and its effects during 1950-2018. *Climate Dynamics*, **60**(7): 1963-1985, https://doi.org/10.1007/s00382-022-06417-8.

Zhang X H, Liang X Z. 1989. A numerical world ocean general circulation model. *Advances in Atmospheric Sciences*, **6**(1): 44-61, https://doi.org/10.1007/BF02656917.

Zheng F, Zhang R-H. 2012. Effects of interannual salinity variability and freshwater flux forcing on the development of the 2007/08 La Niña event diagnosed from Argo and satellite data. *Dynamics of Atmospheres and Oceans*, **57**: 45-57, https://doi.org/10.1016/j.dynatmoce.2012.06.002.

Zheng F, Zhang R-H, Zhu J. 2014. Effects of interannual salinity variability on the barrier layer in the western-central equatorial pacific: a diagnostic analysis from Argo. *Advances in Atmospheric Sciences*, **31**(3): 532-542, https://doi.org/10.1007/s00376-013-3061-8.

Zhi H, Yang Z H, Zhang R-H et al. 2023. Asymmetry of salinity variability in the tropical Pacific during Interdecadal Pacific Oscillation phases. *Advances in Atmospheric Sciences*, **40**(7): 1269-1284, https://doi.org/10.1007/s00376-022-2284-y.

Zhi H, Zhang R-H, Lin P F et al. 2019a. Interannual salinity variability in the tropical Pacific in CMIP5 simulations. *Advances in Atmospheric Sciences*, **36**(4): 378-396, https://doi.org/10.1007/s00376-018-7309-1.

Zhi H, Zhang R-H, Lin P F et al. 2019b. Effects of salinity variability on recent El Niño events. *Atmosphere*, **10**(8): 475, https://doi.org/10.3390/atmos10080475.